RSC Advances

PAPER

View Article Online
View Journal | View Issue

Cite this: *RSC Adv.*, 2025, **15**, 6764

Soxhlet extraction of *Momordica cochinchinensis* fruit peel for β-carotene recovery†

Hai D. Tran, [a] Nguyen Thi Tu Nguyen,[b] Trinh Thu Phuong,[b] Quoc Hai Nguyen [c] and Van-Han Dang *[d]

Received 25th December 2024
Accepted 18th February 2025

DOI: 10.1039/d4ra08999e

rsc.li/rsc-advances

β-Carotene, a potent natural antioxidant, was recovered from the peel of *Momordica cochinchinensis* (gac) fruit peel using Soxhlet extraction. Experimental results indicated that both the sample mass and solvent flow rate exerted a positive influence on the yield of β-carotene. The β-carotene extraction achieved the highest yield with a solvent mixture of ethyl acetate and acetone in a 6 : 4 (v/v) ratio. Thermal stability assessments revealed that β-carotene exhibited greater stability in acetone compared to ethyl acetate under oxygenated conditions. A kinetic model was developed to describe the β-carotene extraction, facilitating the estimation of key parameters including the extraction rate constant, degradation rate constant, and the maximum extractable β-carotene in the gac peel. The model demonstrated good correlation with experimental data, providing valuable insights for optimizing β-carotene extraction protocols.

1. Introduction

β-Carotene is an organic compound belonging to the carotenoid family, distinguished by its vibrant orange-red coloration and its widespread occurrence in plants.[1] As a provitamin A compound, β-carotene plays a crucial role in human health and is widely utilized in the food, pharmaceutical, and cosmetic industries.[2] Its bioactive properties include antioxidant activity, skin protection, potential anticancer effects, and benefits for ocular health.[3,4] Numerous extraction techniques have been employed to isolate β-carotene from plant matrices, including supercritical extraction,[5] ultrasound-assisted extraction,[6] microwave-assisted extraction,[7] pressurized liquid extraction,[8] and conventional solvent extraction.[9]

The Soxhlet apparatus is widely utilized for solid–liquid extraction, offering several advantages, including its ability to handle large sample volumes, elimination of the need for post-extraction filtration, and capacity to accelerate the extraction process.[10,11] While Kongkiatpaiboon and Gritsanapan[12] and Fagbemi *et al.*[13] have successfully employed the Soxhlet apparatus to isolate bioactive compounds from plant materials, the extraction kinetics have not analysed. Several kinetic models proposed to describe the extraction process have been reviewed and discussed by Sridhar *et al.*[14] and Das *et al.*[15] However, a comprehensive mathematical model specifically developed for the Soxhlet extraction method is yet to be reported in the literature.

According to Calvo-Flores *et al.*,[16] ethyl acetate (EA) and acetone (AC) are classified as "Preferred" solvents due to their low toxicity, minimal hazards, and favourable environmental profiles. Additionally, EA and AC are characterized by their availability, low cost, and ease of removal from the extraction solution.[16,17] Consequently, they are commonly utilized for the extraction of valuable bioactive compounds from various biomass sources. The previous studies have reported the successful use of EA for the extraction of β-carotene from tomato,[17,18] citrus peel,[19] and others.[20,21] Similarly, AC has been demonstrated to be an effective solvent for extracting β-carotene from sources such as raw carrots, sweet potatoes, and supplemented chicken meat nuggets,[22] as well as microgreens[23] and sweet potatoes.[24] However, to our knowledge, the extraction of β-carotene from *Momordica cochinchinensis* (gac) peel using a mixture of EA and AC has not been previously investigated. While the solubility of β-carotene in EA (500 mg L^{-1}) is higher than in AC (200 mg L^{-1}),[25] the polarity of AC allows it to disrupt the lipid bilayer of plant cell membranes, potentially enhancing the release of intracellular compounds.[26] The combination of EA and AC may offer a promising strategy to improve the efficiency of β-carotene extraction.

Although gac peel is a rich source of β-carotene, it is frequently discarded as agricultural waste. The present study

[a]*Faculty of Applied Science, Ho Chi Minh University of Natural Resources and Environment, Ho Chi Minh City, Vietnam. E-mail: tdhai@hcmunre.edu.vn*
[b]*Faculty of Applied Sciences, Ton Duc Thang University, Ho Chi Minh City, Vietnam. E-mail: 62000839@student.tdtu.edu.vn; 62000635@student.tdtu.edu.vn*
[c]*Biomaterials and Nanotechnology Research Group, Faculty of Applied Sciences, Ton Duc Thang University, Ho Chi Minh City, Vietnam. E-mail: nguyenquochai@tdtu.edu.vn*
[d]*Laboratory of Biofuel and Biomass Research, Faculty of Chemical Engineering, Ho Chi Minh University of Technology (HCMUT), VNU-HCM, Ho Chi Minh City, Vietnam. E-mail: dvhan@hcmut.edu.vn*

† Electronic supplementary information (ESI) available. See DOI: https://doi.org/10.1039/d4ra08999e

aimed to recover β-carotene from gac peel applying a Soxhlet extraction, employing a solvent mixture of EA and AC. The effects of volume ratio of EA to AC, sample mass, and solvent flow rate on the β-carotene extraction yield were investigated. Furthermore, a mathematical model was developed and simulated to characterize the extraction process in the Soxhlet apparatus.

2. Modeling of Soxhlet extraction

Based on the operational principles, we propose a two-stage Soxhlet extraction process. The first stage, referred to as the filling stage, begins when the first drop of condensed solvent falls and ends when the thimble is fully filled. During this phase, the thimble can be characterized as a semi-batch reactor. The end of the filling stage was represented by "x" points in Fig. 4b, 5b, and 6b. The second stage, known as the cycling stage, begins immediately following the completion of the filling stage. In this phase, the thimble functions as a continuous reactor.

To estimate mathematical equations for describing the kinetic of β-carotene extraction, several assumes were proposed: (i) uniform distribution of β-carotene concentration within the thimble, (ii) a constant rate of condensed solvent, (iii) neglect of solvent loss during sampling, and (iv) the absence of β-carotene in the condensed solvent flow.

2.1. Modelling the filling stage

For modelling the kinetics of Soxhlet extraction, it is assumed that the extraction rate of β-carotene follows a pseudo-homogeneous reaction model. Additionally, previous studies have indicated that the degradation of β-carotene in *n*-decane solvent follows the first-order kinetics.[27] Therefore, the time-dependent concentration of β-carotene in the thimble is expressed by eqn (1).

$$\Re = \frac{\mathrm{d}C_\mathrm{t}}{\mathrm{d}t} = \Re_\mathrm{e} - \Re_\mathrm{d} = k_\mathrm{e}C_\mathrm{s} - k_\mathrm{d}C_\mathrm{t} \tag{1}$$

where $\Re_\mathrm{e} = k_\mathrm{e}C_\mathrm{s}$ and $\Re_\mathrm{d} = k_\mathrm{d}C_\mathrm{t}$ are the extraction rate and degradation rate, respectively, C_s is the apparent concentration of β-carotene, C_t is the concentration of β-carotene in the extract within the thimble, k_e is the extraction rate constant, and k_d is the degradation rate constant. The formula for C_s is defined by eqn (2).

$$C_\mathrm{s} = \frac{m_\mathrm{s}}{V_\mathrm{t}} \tag{2}$$

where m_s is the extractable β-carotene mass from the sample in the thimble at time t and V is the volume of solvent in the thimble at time t. Observably, $m_\mathrm{s} = m_{\mathrm{s,max}}$ at $t = 0$ and $m_\mathrm{s} \rightarrow 0$ when $t \rightarrow \infty$. The mass of β-carotene extracted into the solvent at time t, denoted as m_t, is given by eqn (3).

$$m_\mathrm{t} = m_{\mathrm{s,max}} - m_\mathrm{s} - m_{\mathrm{d}_1} \tag{3}$$

where m_{d_1} is the mass of degraded β-carotene in the thimble.

By combining eqn (2) and (3), eqn (1) can be rewritten as eqn (4).

$$\begin{aligned}\frac{\mathrm{d}C_\mathrm{t}}{\mathrm{d}t} &= k_\mathrm{e}\frac{m_{\mathrm{s,max}} - m_\mathrm{t} - m_{\mathrm{d}_1}}{V_\mathrm{t}} - k_\mathrm{d}\frac{m_\mathrm{t}}{V_\mathrm{t}} \\ &= \frac{k_\mathrm{e}(m_{\mathrm{s,max}} - m_\mathrm{t} - m_{\mathrm{d}_1}) - k_\mathrm{d}m_\mathrm{t}}{V_\mathrm{t}}\end{aligned} \tag{4}$$

Mass balancing for β-carotene in the thimble yields eqn (5).

$$\Re V_\mathrm{t} = \frac{\mathrm{d}m_\mathrm{t}}{\mathrm{d}t} \tag{5}$$

Substituting eqn (4) into eqn (5) results in eqn (6).

$$\frac{\mathrm{d}m_\mathrm{t}}{\mathrm{d}t} = k_\mathrm{e}(m_{\mathrm{s,max}} - m_\mathrm{t} - m_{\mathrm{d}_1}) - k_\mathrm{d}m_\mathrm{t} \tag{6}$$

Degradation rate of β-carotene follows the first-order kinetic, as expressed by eqn (7).

$$\frac{\mathrm{d}m_{\mathrm{d}_1}}{\mathrm{d}t} = k_\mathrm{d}m_\mathrm{t} \tag{7}$$

2.2. Modelling the cycling stage

2.2.1. Operation of thimble. The mass balance for extracted β-carotene in the thimble is given by eqn (8).

$$\frac{\mathrm{d}m_t}{\mathrm{d}t} = -F_\mathrm{out} - \Re V_\mathrm{f} \tag{8}$$

where V_f is the volume of solvent in the thimble at the end of the filling stage ($t = t_\mathrm{f}$), F_out is the mass flow transferring from the thimble into the receiving flask, which can be calculated using eqn (9).

$$F_\mathrm{out} = qC_\mathrm{t} = q\frac{m_\mathrm{t}}{V_\mathrm{f}} = \frac{m_\mathrm{t}}{\tau} \tag{9}$$

where $\tau = V_\mathrm{f}/q$ is called the space time, which is recorded from each experimental run.

By substituting eqn (2) and (9) into eqn (8), the expression can be rewritten as eqn (10).

$$\frac{\mathrm{d}m_\mathrm{t}}{\mathrm{d}t} = -\frac{1}{\tau}m_\mathrm{t} + k_\mathrm{e}(m_{\mathrm{s,max}} - m_\mathrm{t} - m_{\mathrm{d}_1} - m_\mathrm{b} - m_{\mathrm{d}_2}) - k_\mathrm{d}m_\mathrm{t} \tag{10}$$

where m_{d_2} is the mass of the β-carotene degraded in the receiving flask.

2.2.2. Operation of the receiving flask. The mass flow of β-carotene from the thimble to the receiving flask results in the accumulation of β-carotene in the receiving flask. The variation of the mass of β-carotene in the receiving flask can be described by eqn (11).

$$\frac{\mathrm{d}m_\mathrm{b}}{\mathrm{d}t} = qC_\mathrm{t} = q\frac{m_\mathrm{t}}{V_\mathrm{f}} = \frac{1}{\tau}m_\mathrm{t} - k_\mathrm{d}m_\mathrm{b} \tag{11}$$

Eqn (12) presents the kinetic of β-carotene degradation in the receiving flask.

$$\frac{dm_{d_2}}{dt} = k_d m_b \quad (12)$$

where m_b is the mass of β-carotene in the receiving flask.

3. Experimental

3.1. Chemicals and apparatus

Acetone, AC, (99.7%) and ethyl acetate, EA, (99.5%) were obtained from VN-CHEMSOL CO., LTD. Standard β-carotene (96%) was purchased from Shanghai Macklin Biochemical Co., Ltd. All chemicals were used directly without further purification.

The Soxhlet apparatus consists of a three-neck round-receiving flask, a thimble, and a condenser with a heating magnetic stirrer serving as the heat source.

The concentration of β-carotene was determined using an Evolution UV-Vis spectrophotometer (Thermo Fisher Scientific, USA), with measurements taken at the maximum wavelength of 455 nm (as discussed in Section 4.1), 1 cm of path length.

3.2. Preparation of β-carotene solutions for calibration

A stock solution (80 mg L^{-1}) was prepared by dissolving 83.3 mg of the standard β-carotene (96% w/w) into 1000 mL of solvent mixtures containing EA and AC at different volume ratios. Subsequently, the stock solution was then diluted to produce working solutions with concentrations ranging from 0.5 to 5 mg L^{-1}. The volume ratios of EA to AC used were 0 : 10, 3 : 7, 6 : 4, 7 : 3, and 8 : 2.

3.3. Preparation of raw material

A total of 40 kg of fresh gac fruit were purchased from a traditional market in Ho Chi Minh City, Vietnam. The selected fruits need to be similar in terms of peel colour and size. The fruits were thoroughly washed by tap water to remove dirt, pesticide residues, and surface contaminants before cutting. The peels were then sliced into rods with dimensions of 1 × 1 × 6 cm (thickness × width × length) and dried at 100 °C until reaching a dry basis moisture content of 10–15%. The dried gac peel was subsequently ground and sieved through a 1 mm mesh. The obtained material was stored in zipper bags for β-carotene extraction experiments.

3.4. Operation of β-carotene extraction

A Soxhlet apparatus was assembled as illustrated in Fig. 1, using a receiving flask and covering the top of the condenser by a plastic sheet. Initially, 300 mL of solvent was added to the receiving flask. β-Carotene extraction was conducted at different volume ratios of EA to AC, sample masses, and condensed flow rates. At desired time intervals, extracts from the receiving flask were collected to quantify the concentration of β-carotene. The extraction experiments were repeated three times at each condition.

The mass of β-carotene in the receiving flask can calculated based on its concentration in the receiving flask, as expressed in eqn (13).

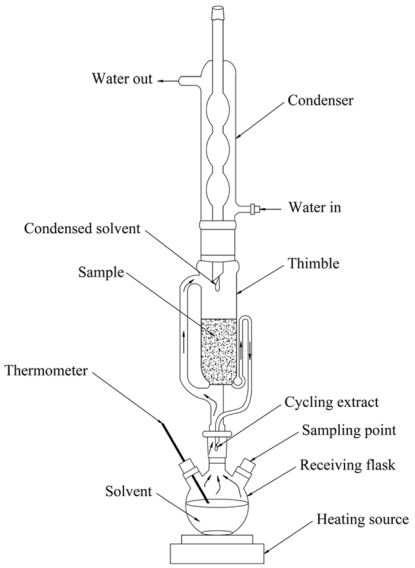

Fig. 1 Scheme of Soxhlet apparatus.

$$m_b = C_b V_b = C_b(V_0 - V_f) \quad (13)$$

where C_b is the concentration of β-carotene in the receiving flask, V_b is the solvent volume in the receiving flask, and V_0 is the initial volume of solvent charged into the receiving flask (V_0 = 0.3 L).

After each extraction run, the heating source was turned off, and the system was allowed to cool down for 30 minutes under ambient conditions. Then, the volume of free solvent (V_g) was determined by transferring it to a graduated cylinder. The volume of the retained solvent (V_h) in the sample bulk was calculated based on the difference between the wet and initial sample masses. Therefore, at the end of the filling stage, the volume of solvent in the thimble and receiving flask could be calculated to be $V_f = V_g + V_h$, and $V_b = V_0 - V_f$, respectively.

3.5. Procedures for the study of β-carotene degradation

To study the degradation of β-carotene in EA under temperature and oxygen conditions, 4 glass bottles (20 mL) containing 10 mL of β-carotene solution (40 mg L^{-1}) were prepared. Each bottle was bubbled with oxygen for 15–20 seconds and then immediately sealed. These oxygen-bubbled bottles were stored at 30 °C. At 0, 1, 2, and 3 hours of storage, one bottle was removed at each time point, and the remaining β-carotene concentration was analysed. Similar experimental procedures were conducted at 60 °C to evaluate the stability of β-carotene at elevated temperatures.

Similar procedures were again performed for AC solvent.

3.6. Numerical method

To determine the values of kinetic parameters (k_d, k_e, $m_{s,max}$) using Soxhlet apparatus, the developed model was fitted with experimental data for the cycling stage. As outlined in Section 2.2, the system of eqn (7), (10)–(12) was numerically solved

using a 4th order Runge–Kutta method, revealing the relationship between m_b and t with conditions:

$$\begin{cases} m_t = 0 \quad \text{at } t = 0 \\ m_{d_1} = 0 \quad \text{at } t = 0 \\ m_b = 0 \quad \text{with } 0 \le t \le t_f \\ m_{d_2} = 0 \quad \text{with } 0 \le t \le t_f \end{cases}$$

The least squares method was employed to minimize the sum of squared errors (SSE) using Solver-Excel tool with Generalized Reduced Gradient method.

$$\text{SSE} = \sum (m_{b,cal} - m_{b,exp})_i^2 \rightarrow \min \quad (14)$$

where $m_{b,cal}$ and $m_{b,exp}$ are mass of β-carotene from calculation and experiment, respectively.

To evaluate the goodness of fit between the model and experimental data, the squared correlation coefficient (R^2) is used, where $0 \le R^2 \le 1$. R^2 is defined as eqn (15).

$$R^2 = 1 - \frac{\text{SSE}}{\text{TSS}} \quad (15)$$

where TSS is the total sum of squares, which is calculated by eqn (16).

$$\text{TSS} = \sum \left(m_{b,exp} - \overline{m_{b,exp}} \right)^2 \quad (16)$$

where $\overline{m_{b,exp}}$ is the mean of experimental results.

3.7. Determination of β-carotene concentration in receiving flask

As detailed in Section 4.1, the light absorbance of β-carotene is influenced by both its concentration and the volume ratio of EA to AC, denoted as r. The r value within the receiving flask can be computed using eqn (A-5), derived from the combination of Raoult's law and the Antoine equations (as elaborated in the Appendix). All physicochemical properties of the pure solvents were measured at the temperature of the extract within the receiving flask.

The margin of error (MoE) for mean concentration was calculated by eqn (17).

$$\text{MoE} = t_{\alpha/2} \frac{\text{SD}}{\sqrt{n}} \quad (17)$$

where $t_{\alpha/2}$ represents the value from the Student's t-distribution at a confidence coefficient of 0.95 with $n - 1 = 2$ degrees of freedom, SD denotes the standard deviation, and $n = 3$ indicates the number of times the experiment was repeated.

4. Results and discussion

4.1. Behaviour of UV-vis absorbance of β-carotene in ethyl acetate and acetone

The analysis of UV-vis absorbance provides valuable insights for evaluating both the quantity and quality of β-carotene. Fig. 2a illustrates the absorbance spectra for standard β-carotene at

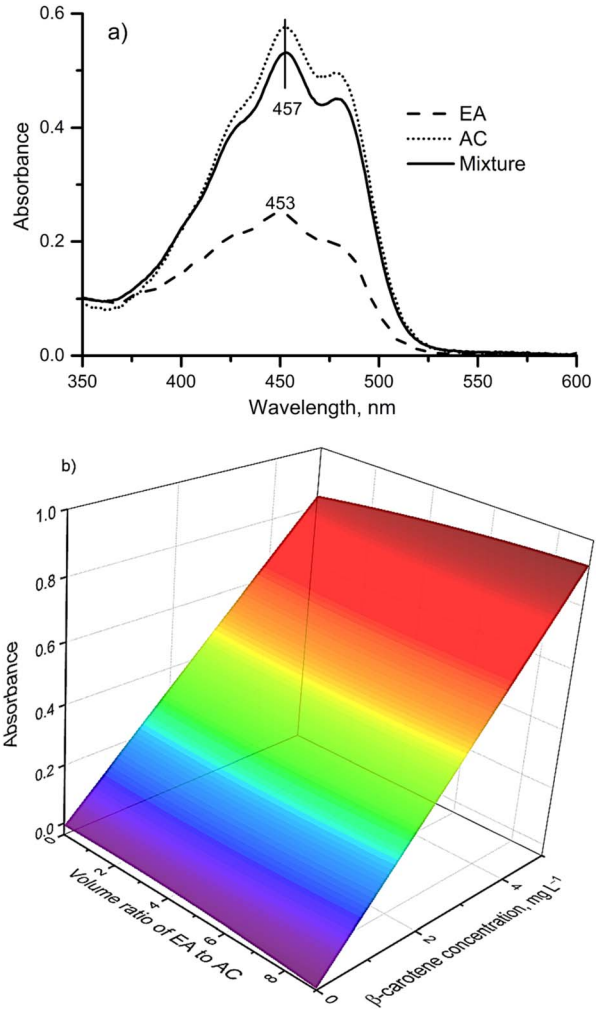

Fig. 2 The response of β-carotene to UV-vis radiation in different solvents: (a) absorbance spectra and (b) calibration surface.

a concentration of 3 mg L^{-1} in EA, AC, and a mixture of EA and AC (7 : 3 vol/vol). It is apparent that the solvent employed significantly influences the absorbance of β-carotene. The principal mechanism behind the absorbance of light by β-carotene is the electronic transition from the ground state to the excited state, which occurs within the conjugated double bonds of the molecule. This transition gives rise to a pronounced absorbance peak at the maximum wavelength (λ_{max}).[28] Changes in the electronic field surrounding β-carotene can alter this transition, resulting in shifts in both the position and intensity of the absorption peak. As β-carotene has a conjugated π-electron system, it exhibits electron-donating properties,[29] which enable interactions with electron-accepting molecules such as the solvents EA and AC *via* donor–acceptor interactions. In the case of AC, the solvent's higher acceptor number[30] results in the destabilization of the ground state of π-electron in β-carotene and stabilization of its excited state, which leads to distinct effects on β-carotene's electronic states. Additionally, the molar absorptivity of β-carotene in AC is greater than in EA.[25] As a result, the presence of AC not only shifts the λ_{max} to longer

Table 1 Obtained constants in calibration surface function (eqn (18))

Constants	Value
a	-8.66×10^{-3}
b_1	0.17
b_2	2.42×10^{-3}
b_{11}	-1.08×10^{-4}
b_{22}	-6.02×10^{-4}
b_{12}	2.51×10^{-3}

wavelengths but also increases the intensity of the absorbance peak, as shown in Fig. 2a. However, the shift in λ_{max} observed in this study remains relatively narrow, ranging from 453 to 457 nm. Given the minimal shift in peak position, an average λ_{max} value of 455 nm was selected for subsequent quantitative analysis of β-carotene in the samples.

As previously discussed, the absorbance of β-carotene is influenced by the solvent. Therefore, a mathematical relationship (eqn (18)) was derived to describe the dependence of the maximum absorbance (A_{max}) on both the concentration of β-carotene (C) and volume ratio of EA to AC (r). This equation was employed to quantify the β-carotene content in the extracts.

$$A_{max} = a + b_1C + b_2r + b_{11}C^2 + b_{22}r^2 + b_{12}Cr \quad (18)$$

where a, b_1, b_2, b_{11}, b_{22}, and b_{12} are constants.

Regression analysis of eqn (18) using experimental data yielded the constants, as listed in Table 1, corresponding to the three-dimensional surface depicted in Fig. 2b, called calibration surface. The experimental and predicted values indicated a good agreement ($R^2 = 0.9579$, p-value < 0.0001) according to the analysis of variance.

4.2. Validation of β-carotene degradation

This study examined the stability of β-carotene in EA and AC solvents under the influence of temperature and oxygen. Fig. 3 presents the reduction of β-carotene in both solvents at 30 °C and 60 °C. It can overall be observed that β-carotene exhibited greater stability at 30 °C compared to 60 °C.

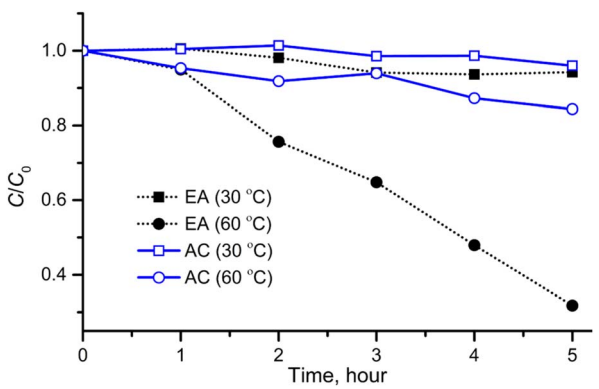

Fig. 3 Degradation of β-carotene in EA and AC at 30 and 60 °C.

At 30 °C, β-carotene demonstrated remarkable stability in both EA and AC. After 3 hours of storage, minimal degradation, approximately 6% and 2% of the initial β-carotene reduced in EA and AC, respectively, was observed. However, as the temperature increased to 60 °C, the degradation of β-carotene was significantly accelerated. After 3 hours at 60 °C, β-carotene in EA experienced a degradation of approximately 35%, which was six times greater than the degradation observed at 30 °C. In contrast, the degradation in AC at 60 °C was less pronounced, with about 7% of the initial BC reduced after 3 hours. These results indicate that temperature is the key factor influencing the degradation of β-carotene. Additionally, the degradation of β-carotene in AC was less sensitive to temperature changes than in EA.

High temperature promotes the processes that occur during extraction, including degradation. The conjugated π-electron system within the polyene chain of β-carotene has been implicated as a key factor contributing to its degradation.[31] Due to its ability to participate in electron transfer reactions,[31] β-carotene can interact with peroxyl radicals to form β-carotene radical cations.[32] These radical cations can subsequently react with oxygen or undergo self-decomposition.[33] In another way, β-carotene can directly react with oxygen through autoxidation.[34] These mechanisms contribute to the accelerated degradation of β-carotene in EA. However, the formation of β-carotene radical cations is less likely to occur in AC.[35] Consequently, β-carotene degradation in AC is primarily attributed to autoxidation *via* singlet oxygen quenching.[36] These findings offer a valuable foundation for developing kinetic models and interpreting experimental results for β-carotene extraction from gac peel.

4.3. Soxhlet extraction of β-carotene

4.3.1. Effect of volume ratio of ethyl acetate to acetone. Initially, the influence of the volume ratio (r) of EA to AC on the extraction of β-carotene from gac peel was systematically investigated. For each extraction trial, a constant total solvent volume of 300 mL was used in conjunction with 26 g of sample. The experimental procedure revealed that the time required for the filling stage was consistent across varying r values, averaging approximately 15 minutes. The time-dependent accumulation of β-carotene in the receiving flask during the extraction process is shown in Fig. 4a. The data demonstrated that the combination of EA and AC solvents significantly enhanced the efficiency of β-carotene extraction. As the r was increased from 0 : 10 to 6 : 4, a corresponding increase in the mass of β-carotene extracted was observed. However, when the ratio was further elevated beyond 6 : 4, the extraction efficiency declined, indicating a diminishing return on β-carotene yield with higher r values. Based on these findings, the optimal r value for maximizing β-carotene extraction from gac peel was determined to be 6 : 4.

EA and AC solvents have been proposed to enhance the extraction of β-carotene in different pathways. β-Carotene, a nonpolar compound, is primarily synthesized and stored within plastids, which are organelles enclosed in plant cells.[37] Due to its polar nature, AC is capable of interacting with the lipid bilayer of the cell membrane, leading to the leakage of

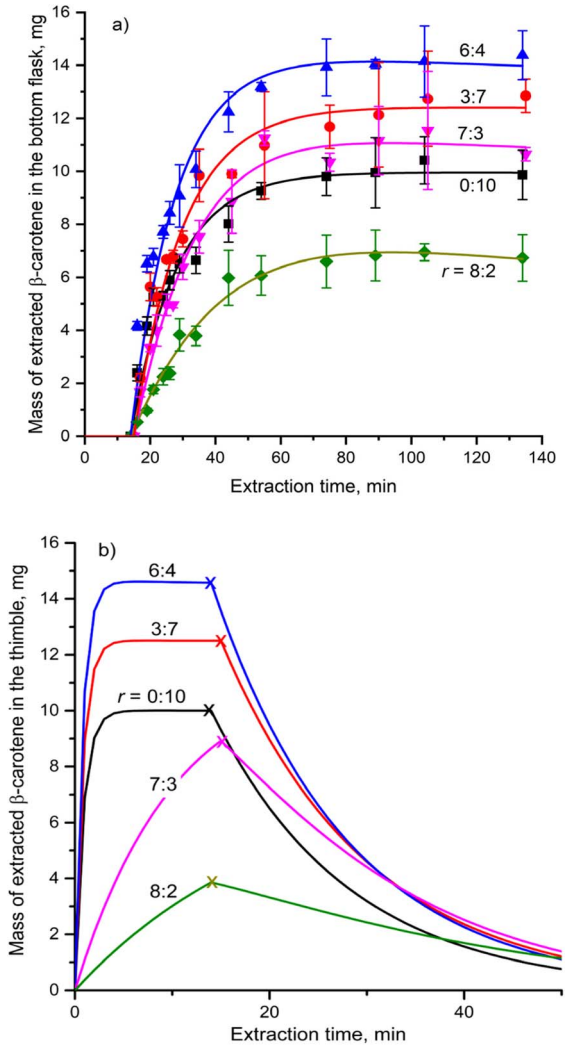

Fig. 4 Mass of β-carotene in (a) the receiving flask and (b) the thimble at different volume ratios of EA to AC (m_0 = 26 g, q = 8.64 mL min^{-1}).

cellular contents.[38] Meanwhile, β-carotene exhibits higher solubility in the medium-polar EA solvent (12.06 mg mL^{-1} at 50 °C) compared to the more polar AC solvent (1.82 mg mL^{-1} at 50 °C).[39] As a result, the polarity difference between these solvents creates a favorable concentration gradient for β-carotene extraction when using EA. The combination of EA and AC solvents, with distinct polarities, thus enhances the extraction of β-carotene by leveraging their complementary properties. This approach has been successfully applied in various extraction systems, including β-carotene extraction from orange peel using acetone/hexane mixtures,[40] from the aril oil of gac using methanol/chloroform mixtures,[41] and from maize using methanol/ethyl acetate mixtures.[42]

The smooth curves presented in Fig. 4a and b represent the simulated temporal variations in the mass of β-carotene within the receiving flask and thimble, respectively. As shown in Fig. 4b, during the filling stage, the β-carotene mass in the thimble increases rapidly, approaching an equilibrium value before exhibiting an exponential decrease during the cycling stage for the r ranging from 0 : 10 to 6 : 4. However, for r values of 7 : 3 and 8 : 2, the β-carotene mass in the thimble did not reach a plateau during the filling stage. At these ratios, AC may not be enough for its lipid bilayer disruption role, leading to more requiring time for extraction processes.

The r has a significant influence on the rate constants governing the extraction and degradation of β-carotene, as shown in Table 2. Notably, the extraction rate constant (k_e) is significantly higher than the degradation rate constant (k_d). As the r parameter increased from 0 : 10 to 6 : 4, a corresponding increase in the k_e was observed, suggesting that EA plays a critical role in enhancing β-carotene extraction efficiency. This enhancement can be attributed to the higher solubility of β-carotene in EA, which creates a more favourable concentration gradient between the β-carotene stored in the plant cells and the solvent. This gradient facilitates the transfer of β-carotene from the cell interior to the solvent phase, enhancing the overall extraction process. In contrast, at the higher r values of 7 : 3 and 8 : 2, the proportion of AC in the solvent mixture may be insufficient to effectively disrupt the cell membranes, resulting in reduced solvent's penetrability and a subsequent decrease in k_e.

As depicted in Table 2, a positive correlation exists between the r and k_d. However, the precise mechanism underlying the observed increase in k_d with rising r remains unclear. β-Carotene is known to undergo autoxidation in the presence of free oxygen, leading to the formation of degradation products. Specifically, in the presence of AC, β-carotene typically yields carbonyl compounds,[43] while in EA, β-carotene tends to form copolymers.[44] Previous studies have indicated that dissolved oxygen in non-polar solvents such as *n*-decane can significantly influence β-carotene autoxidation, but the formation of carbonyl products was not reported.[27] More recently, endoperoxides have been identified as the major reaction products resulting from the interaction between oxygen and β-carotene.[45] While free oxygen is a recognized factor in β-carotene

Table 2 Calculated kinetic parameters of the β-carotene extraction from gac peel at different volume ratios of EA to AC

	Volume ratios of EA to AC				
Parameters	0 : 10	3 : 7	6 : 4	7 : 3	8 : 2
k_e (min^{-1})	1.22	1.37	1.54	9.80×10^{-2}	4.64×10^{-2}
k_d (min^{-1})	4.08×10^{-5}	6.04×10^{-5}	3.46×10^{-4}	5.15×10^{-4}	1.73×10^{-3}
$m_{s,max}$ (mg)	10.00	12.51	14.64	11.64	8.18
R^2	0.9518	0.9611	0.9496	0.9834	0.9867

degradation, the relationship between free oxygen and EA and the possibility of a direct interaction between β-carotene and EA remains to be elucidated.

The predicted maximum extractable masses of β-carotene ($m_{s,max}$), derived from the proposed model, show close agreement with the experimental result. Additionally, the high R^2 coefficients suggest that the model is highly effective in describing the extraction of β-carotene from gac peel using a Soxhlet apparatus.

4.3.2. Effects of sample mass. During the extraction process, continuous solvent reflux was employed to ensure that the solvent in the thimble remained below the saturation point of β-carotene, thereby maintaining a consistent and effective driving force for the extraction process, irrespective of sample mass (m_0). As shown in Fig. 4a, an increase in sample mass from 13 to 52 g resulted in a corresponding increase in the amount of β-carotene extracted. After 120 minutes of the cycling stage, the β-carotene yield per gram of sample was determined to be 0.58, 0.55, and 0.51 mg g^{-1} for 13, 26, and 52 g of sample masses, respectively. These findings indicate that, within the range studied, the β-carotene extraction yield remains relatively independent of sample mass. Based on these results, the maximum sample mass capacity of the thimble, 52 g, was selected for subsequent experiments to optimize the extraction process.

The increase in the sample mass within the thimble resulted in a decreased solvent capacity, leading to a slightly shorter filling time, as recorded from the experimental runs. By fitting the proposed model to experimental data, smooth curves representing the time-dependent extraction of β-carotene mass in the receiving flask (Fig. 5a) and the thimble (Fig. 5b) were generated. The corresponding parameters were determined and presented in Table 3. AC has a lower boiling point than EA, leading to AC filling the void spaces within the thimble following EA. Increasing sample mass reduces this void space. Therefore, a large sample mass causes the shortage of EA in the thimble, declining the role of EA. As a result, the k_e at a sample mass of 52 g was slightly lower than that at 13 and 26 g.

Previous studies have demonstrated that β-carotene is particularly vulnerable to degradation in the presence of oxygen.[46] The Soxhlet extraction system utilized in this study operated under atmospheric conditions, which allowed oxygen to diffuse into the void spaces of the sample. An increase in sample mass resulted in a greater pressure drop across the material,[47] which in turn impeded the escape of oxygen from the sample. This restriction on oxygen diffusion promoted the degradation of β-carotene,[48] as evidenced by the gradual increase in k_d with sample mass (Table 3). However, the overall k_d values remained substantially lower than the k_e, indicating that β-carotene degradation had a comparatively minor effect on the overall extraction efficiency.

As shown in Fig. 5b, a larger sample mass caused the higher mass of β-carotene remaining in the thimble, suggesting that more time was required to transfer β-carotene from the thimble to the receiving flask. However, despite this delay, the β-carotene content in the thimble consistently approached zero by the conclusion of each extraction cycle. This suggests that a 120-minute cycling stage was sufficient to achieve near-complete extraction of β-carotene from gac peel. This finding is consistent with the previously observed independence of β-carotene yield from sample mass.

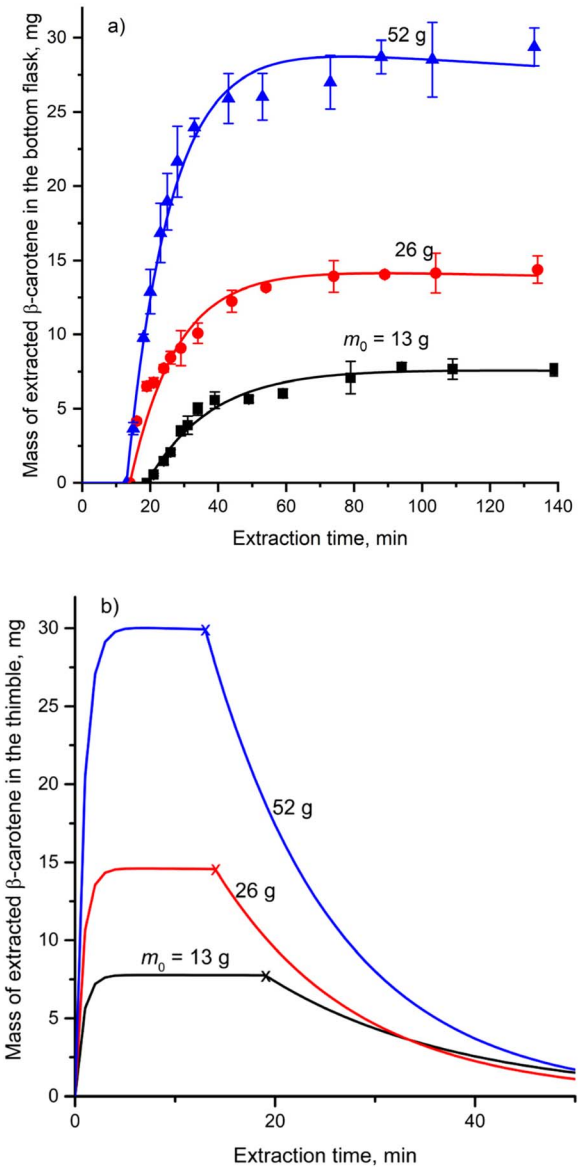

Fig. 5 Mass of β-carotene in (a) the receiving flask and (b) the thimble at different sample masses (r = 6 : 4, q = 8.64 mL min^{-1}).

Table 3 Calculated kinetic parameters of the β-carotene extraction from gac peel at different sample masses

	Sample masses (g)		
Parameters	13	26	52
k_e (min^{-1})	1.50	1.54	1.32
k_d (min^{-1})	2.00×10^{-4}	3.45×10^{-4}	5.59×10^{-4}
$m_{s,max}$ (mg)	7.79	14.64	28.01
R^2	0.9764	0.9496	0.9973

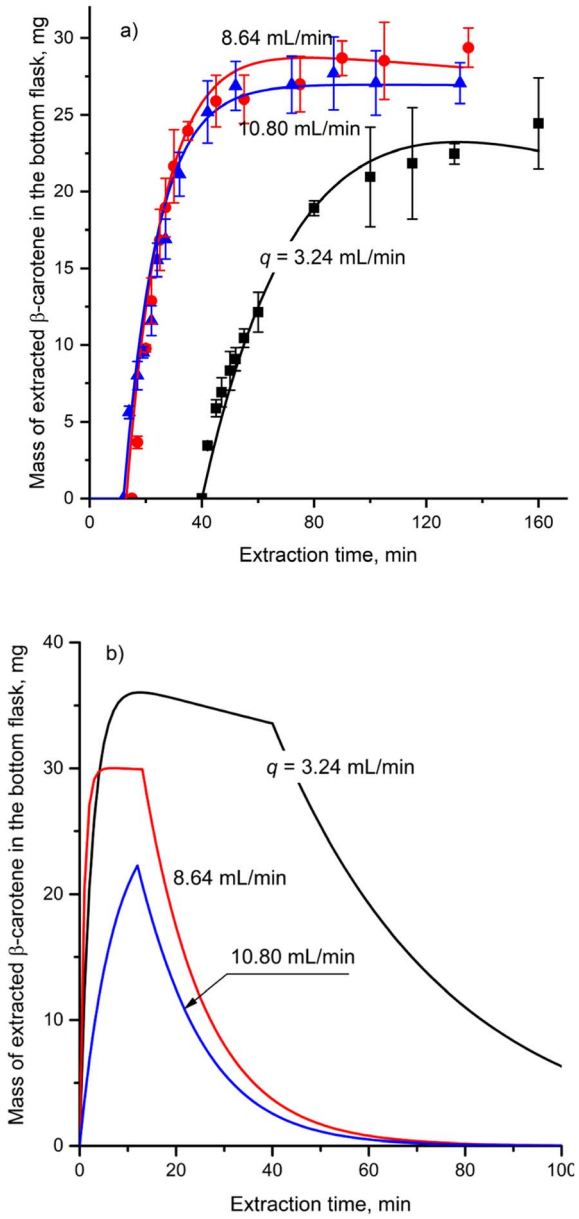

Fig. 6 Mass of β-carotene in (a) the receiving flask and (b) the thimble at different condensed solvent flow rates ($r = 6:4$, $m_0 = 52$ g).

4.3.3. Effect of condensed solvent flow rate. To investigate the influence of condensed flow rate (q) on the extraction of β-carotene from gac peel, heat power was adjusted to three levels corresponding to q values of 3.24, 8.64, and 10.80 mL min^{-1}. As illustrated in Fig. 6a, an increase in q resulted in a shorter filling stage and a faster rate of β-carotene extraction. Represented by the smooth curves in Fig. 6a, the simulation result shows the most pronounced convex curve at a q of 3.24 mL min^{-1}, likely due to the contribution of β-carotene degradation during the extraction process. At q of 8.64 and 10.80 mL min^{-1}, the β-carotene mass in the receiving flask reached a plateau and did not exhibit a decline phase. However, the β-carotene extractability at $q = 8.64$ mL min^{-1} was not significantly different from that at $q = 10.80$ mL min^{-1}, indicating that a q value higher than 8.64 mL min^{-1} did not promote β-carotene extraction efficiency.

Table 4 Calculated kinetic parameters of the β-carotene extraction from gac peel at different condensed solvent flow rates

	Condensed solvent flow rates (mL min^{-1})		
Parameters	3.24	8.64	10.80
k_e (min^{-1})	0.40	1.20	2.69
k_d (min^{-1})	2.85×10^{-3}	5.29×10^{-4}	4.34×10^{-5}
$m_{s,max}$ (mg)	37.36	30.12	27.10
R^2	0.9772	0.9888	0.9718

Fig. 6b demonstrates a significant influence of q on the kinetics of β-carotene within the thimble. During the filling stage, the mass of β-carotene in the thimble exhibited the sign of decline at a q of 3.24 mL min^{-1} and did not attain a plateau at a q of 10.80 mL min^{-1}. In the cycling stage, an increase in q resulted in a decreased retention time of the solvent within the thimble, thereby accelerating the withdrawal rate of β-carotene from the thimble.

The parameters presented in Table 4 were obtained by fitting the proposed model to the experimental data. At higher q, the β-carotene extracted in the thimble is rapidly transferred to the receiving flask, creating a steep concentration gradient of β-carotene between the gac peel particles and the solvent within the thimble. This rapid transfer enhances the extraction efficiency, leading to an increase in the k_e with increasing q. A similar trend has been reported for soybean oil extraction using a percolation-type extractor.[49] Additionally, at elevated q values, the void space within the thimble is quickly filled, which minimizes the exposure time of the extracted β-carotene to the oxygen present in the sample. This reduction in exposure to oxygen limits β-carotene degradation, resulting in a decrease in the k_d value.

5. Conclusions

This study successfully recovered β-carotene from gac peel using Soxhlet extraction. The effects of volume ratio of EA to AC, sample mass, and condensed solvent flow rate on the β-carotene extractability have been explored. Additionally, the influence of temperature on β-carotene degradation under oxygenated conditions was evaluated, revealing that β-carotene exhibited greater stability in AC compared to EA. Experimental results demonstrated that β-carotene extraction efficiency was highest at a 6 : 4 volume ratio of EA to AC and that β-carotene yield increased with sample mass and condensed flow rate. A mathematical model describing the β-carotene extraction process was developed, allowing for the determination of important kinetic parameters. The developed model exhibited good consistency with experimental data through the closeness of R^2 to 1. Overall, the extraction rate constant was significantly greater than the degradation rate constant. The maximum extractable β-carotene amount in gac peel depends on operating conditions. This study demonstrates the feasibility of β-

carotene extraction from gac peel and provides valuable insights into the kinetics of β-carotene extraction, offering potential avenues for optimization and application.

Data availability

The data supporting this article have been included as part of the ESI.†

Author contributions

Hai D. Tran designed the experiments and drafted the manuscript. Nguyen Thi Tu Nguyen performed experiments. Trinh Thu Phuong prepared materials and set up experimental equipment. Quoc Hai Nguyen reviewed and revised the manuscript. Van-Han Dang was responsible for supervision, writing – review and editing.

Conflicts of interest

There are no conflicts to declare.

Appendix

The volume ratio of EA to AC was calculated using eqn (A-1).

$$r = \frac{V_{EA}}{V_{AC}} = \frac{m_{EA}/\rho_{EA}}{m_{AC}/\rho_{AC}} = \frac{n_{EA}}{n_{AC}}\frac{M_{EA}}{\rho_{EA}}\frac{\rho_{AC}}{M_{AC}} \quad \text{(A-1)}$$

where V, m, n, ρ, M are volume, mass, mole, density, and molecular weight of each pure solvent.

Rearranging eqn (A-1), the mole of AC can be determined by eqn (A-2).

$$n_{AC} = \frac{n_{EA}}{r}\frac{M_{EA}}{\rho_{EA}}\frac{\rho_{AC}}{M_{AC}} \quad \text{(A-2)}$$

This leads to eqn (A-3), which can be used to calculate the mole fraction of EA (x_{EA}) in a liquid EA–AC mixture.

$$x_{EA} = \frac{n_{EA}}{n_{EA}+n_{AC}} = \frac{1}{1+\frac{1}{r}\frac{M_{EA}}{\rho_{EA}}\frac{\rho_{AC}}{M_{AC}}} \quad \text{(A-3)}$$

Total vapour pressure at equilibrium state is related to the mole fraction according to Raoult's law, as expressed in eqn (A-4).

$$p = x_{EA}p^*_{EA} + (1-x_{EA})p^*_{AC} \quad \text{(A-4)}$$

where p^*_{EA} and p^*_{AC} are the equilibrium vapour pressures of EA and AC, respectively, which are correlate to temperature by the Antoine equations: $p^* = 10^{A-\frac{B}{T+C}}$. By submitting eqn (A-3) and the Antoine equations into eqn (A-4), we obtain eqn (A-5).

$$p = \frac{1}{1+\frac{1}{r}\frac{M_{EA}}{\rho_{EA}}\frac{\rho_{AC}}{M_{AC}}}\left(10^{A-\frac{B}{T+C}}\right)_{EA} + \left(1-\frac{1}{1+\frac{1}{r}\frac{M_{EA}}{\rho_{EA}}\frac{\rho_{AC}}{M_{AC}}}\right)\left(10^{A-\frac{B}{T+C}}\right)_{AC} \quad \text{(A-5)}$$

where $p = 760$ mmHg is the operation pressure; A, B, and C are Antoine coefficients for the pure solvents, as listed in Table 5; T is the temperature (°C).

Table 5 Antoine coefficients for EA and AC

Antoine coefficients	EA	AC
A	7.25963	7.31414
B	1338.46	1315.67
C	228.608	240.479
Temp. ranges	−83.55 to 250.15	−94.7 to 235.05

Acknowledgements

We acknowledge Ho Chi Minh City University of Technology (HCMUT), VNU-HCM for supporting this study.

References

1 K. Gul, A. Tak, A. K. Singh, P. Singh, B. Yousuf and A. A. Wani, *Cogent Food Agric.*, 2015, **1**, 1018696.
2 Y. Li, Y. Zhao, H. Zhang, Z. Ding and J. Han, *Molecules*, 2024, **29**, 967.
3 T. Grune, G. Lietz, A. Palou, A. C. Ross, W. Stahl, G. Tang, D. Thurnham, S.-a. Yin and H. K. Biesalski, *J. Nutr.*, 2010, **140**, 2268S–2285S.
4 R. Anand, L. Mohan and N. Bharadvaja, *Rev. Bras. Farmacogn.*, 2022, **32**, 491–501.
5 A. S. Patel, A. Kar, S. Dash and S. K. Dash, *Sci. Rep.*, 2019, **9**, 19266.
6 M. Umair, S. Jabbar, M. M. Nasiru, Z. Lu, J. Zhang, M. Abid, M. A. Murtaza, M. Kieliszek and L. Zhao, *Molecules*, 2021, **26**, 6763.
7 A. Elik, D. K. Yanık and F. Göğüş, *Food Sci. Technol.*, 2020, **123**, 109100.
8 A. Mustafa, L. M. Trevino and C. Turner, *Molecules*, 2012, **17**, 1809–1818.
9 H. V. Chuyen, P. D. Roach, J. B. Golding, S. E. Parks and M. H. Nguyen, *Int. J. Food Sci. Technol.*, 2017, **52**, 972–980.
10 N. Fidalgo-Used, E. Blanco-González and A. Sanz-Medel, *Anal. Chim. Acta*, 2007, **590**, 1–16.
11 X. Yu, X. Tu, L. Tao, J. Daddam, S. Li and F. Hu, *J. Funct. Foods*, 2023, **111**, 105868.
12 S. Kongkiatpaiboon and W. Gritsanapan, *Ind. Crops Prod.*, 2012, **41**, 371–374.

13 K. O. Fagbemi, D. A. Aina and O. O. Olajuyigbe, *Sci. World J.*, 2021, **2021**, 1–8.
14 A. Sridhar, M. Ponnuchamy, P. S. Kumar, A. Kapoor, D.-V. N. Vo and S. Prabhakar, *Environ. Chem. Lett.*, 2021, **19**, 3409–3443.
15 I. Das and A. Arora, *Food Hydrocolloids*, 2021, **120**, 106931.
16 F. G. Calvo-Flores, M. J. Monteagudo-Arrebola, J. A. Dobado and J. Isac-García, *Top. Curr. Chem.*, 2018, **376**, 18.
17 K. Szabo, B.-E. Teleky, F. Ranga, I. Roman, H. Khaoula, E. Boudaya, A. B. Ltaief, W. Aouani, M. Thiamrat and D. C. Vodnar, *Molecules*, 2022, **27**, 3771.
18 M. M. Calvo, D. Dado and G. Santa-María, *Eur. Food Res. Technol.*, 2006, **224**, 567–571.
19 Y. Sun, D. Liu, J. Chen, X. Ye and D. Yu, *Ultrason. Sonochem.*, 2010, **18**, 243–249.
20 L. Hladnik, F. A. Vicente, M. Grilc and B. Likozar, *Biomass Convers. Biorefin.*, 2022, **14**, 8459–8467.
21 E. Papaioannou, T. Roukas and M. Liakopoulou-Kyriakides, *Prep. Biochem. Biotechnol.*, 2008, **38**, 246–256.
22 A. K. Biswas, J. Sahoo and M. K. Chatli, *Food Sci. Technol.*, 2011, **44**, 1809–1813.
23 V. M. Paradiso, M. Castellino, M. Renna, P. Santamaria and F. Caponio, *Foods*, 2020, **9**, 459.
24 C.-Y. Lien, C.-F. Chan, C.-L. Huang, Y.-C. Lai and W. C. Liao, *Int. J. Food Eng.*, 2012, **8**, 21.
25 N. E. Craft and J. H. Soares, *J. Agric. Food Chem.*, 1992, **40**, 431–434.
26 H. M. Amaro, F. Fernandes, P. Valentão, P. B. Andrade, I. Sousa-Pinto, F. X. Malcata and A. C. Guedes, *Mar. Drugs*, 2015, **13**, 6453–6471.
27 A. Takahashi, N. Shibasaki-Kitakawa and T. Yonemoto, *J. Am. Oil Chem. Soc.*, 1999, **76**, 897–903.
28 P. O. Andersson, T. Gillbro, L. Ferguson and R. J. Cogdell, *Photochem. Photobiol.*, 1991, **54**, 353–360.
29 V. G. Mairanovsky, A. A. Engovatov, N. T. Ioffe and G. I. Samokhvalov, *J. Electroanal. Chem.*, 1975, **66**, 123–137.
30 K. Burger, B. Zelei, G. Szánthoó-Horváth, T. T. Binh and J. Inorg, *Nucl. Chem.*, 1971, **33**, 2573–2582.
31 C. S. Boon, D. J. McClements, J. Weiss and E. A. Decker, *Crit. Rev. Food Sci. Nutr.*, 2010, **50**, 515–532.
32 N. I. Krinsky and K.-J. Yeum, *Biochem. Biophys. Res. Commun.*, 2003, **305**, 754–760.
33 K. Jomová, O. Kysel, J. C. Madden, H. Morris, S. J. Enoch, S. Budzak, A. J. Young, M. T. D. Cronin, M. Mazur and M. Valko, *Chem. Phys. Lett.*, 2009, **478**, 266–270.
34 R. C. Mordi, J. C. WaIton, G. W. Burton, L. Hughes, K. U. Ingold, D. A. Lindsay and D. J. Moffatt, *Tetrahedron*, 1993, **49**, 911–928.
35 K. M. Haila, B. R. Nielsen, M. I. Heinonen and L. H. Skibsted, *Z. Lebensm.-Unters. Forsch.*, 1997, **204**, 81–87.
36 J. Terao, Y. Minami and N. Bando, *J. Clin. Biochem. Nutr.*, 2010, **48**, 57–62.
37 T. Sun, S. Rao, X. Zhou and L. Li, *Mol. Hortic.*, 2022, **2**, 3.
38 Y. O. Posokhov and A. Kyrychenko, *Comput. Biol. Chem.*, 2013, **46**, 23–31.
39 M. V. Três, E. Francheschi, G. R. Borges, C. Dariva, F. d. C. Corazza, J. V. Oliveira and M. L. Corazza, *Food Sci. Technol.*, 2007, **27**, 737–743.
40 A. Ghazi, *Nahrung*, 1999, **43**, 274–277.
41 J. Kubola, N. Meeso and S. Siriamornpun, *Food Res. Int.*, 2011, **50**, 664–669.
42 S. Rivera and R. Canela, *Molecules*, 2012, **17**, 11255–11268.
43 G. J. Handelman, F. J. G. M. Van Kuijk, A. Chatterjee and N. I. Krinsky, *Free Radicals Biol. Med.*, 1991, **10**, 427–437.
44 T. J. Mogg and G. W. Burton, *Can. J. Chem.*, 2021, **99**, 751–762.
45 M. Zbyradowski, M. Duda, A. Wisniewska-Becker, Heriyanto, W. Rajwa, J. Fiedor, D. Cvetkovic, M. Pilch and L. Fiedor, *Nat. Commun.*, 2022, **13**, 2474.
46 L. K. Henry, N. L. Puspitasari-Nienaber, M. Jarén-Galán, R. B. Van Breemen, G. L. Catignani and S. J. Schwartz, *J. Agric. Food Chem.*, 2000, **48**, 5008–5013.
47 R. K. Padhi, D. T. K. Dora, Y. K. Mohanty, G. K. Roy and B. Sarangi, *Cogent Eng.*, 2016, **3**, 1181821.
48 A. F. Stefanovich and M. Karel, *J. Food Process. Preserv.*, 1982, **6**, 227–242.
49 D. D. Shejawale, C. S. Murugesh, N. K. Rastogi and R. Subramanian, *J. Food Technol.*, 2022, **59**, 4723–4730.